

## ***In Vivo* Imaging of Signal Decay due to Diffusion in the Internal Field in Human Knee Trabecular Bone**

Eric Sigmund<sup>1</sup>, Ravinder Regatte<sup>1</sup>, Mark Schweitzer<sup>1</sup>,  
Hyungjoon Cho<sup>2</sup>, Yi-Qiao Song<sup>3</sup>

<sup>1</sup> Department of Radiology, New York University, New York, NY USA

<sup>2</sup> Memorial Sloan-Kettering Cancer Center, New York, NY USA

<sup>3</sup> Schlumberger-Doll Research, Cambridge, MA USA

Corresponding author: Eric Sigmund, Dept. of Radiology, New York University, New York, NY 10016, E-Mail: eric.sigmund@nyumc.org

(received 22 July 2008, accepted 4 March 2009)

### **Abstract**

This study presents the first demonstration of the MR signal decay due to diffusion in the internal field (DDIF) for *in vivo* knee trabecular bone imaging. DDIF contrast was compared with high resolution FLASH,  $T_1$ , and  $T_2^*$  mapping in healthy volunteers. DDIF maps showed spatial variation, superimposed on a  $T_1$  background, reflecting trabecular structure. DDIF and  $T_2^*$  maps showed correlated contrast near dense trabeculae, but their spatial textures differed, suggesting distinct structural sensitivities.

### **Keywords**

Trabecular bone, internal field, diffusion,  $T_2^*$ , DDIF

### **1. Introduction**

Trabecular bone (TB) consists of a network of plates and rods with thicknesses of  $\sim 100$   $\mu\text{m}$  and spacings of up to 1 mm, located near joints and load-bearing areas of the skeleton (vertebrae, femur, tibia). TB architecture plays a crucial role in mechanical competence and fracture risk, and it remodels to optimally support applied load, according to Wolff's Law [1]. Remodelling can malfunction due to age, inactivity, or hormonal imbalance and lead to weakening. The microstructure of trabecular bone is thus crucially important for diagnosis of pathologies like osteoporosis. However, the standard clinical diagnostic for bone competence remains limited to bone density. While density is undeniably important, it is an inadequate sole predictor of strength. A wide range of MR techniques have thus been developed to provide sensitivity to bone architecture, such as linewidth mapping ( $1/T_2^*$ ) [2], distant dipolar field [3], and high resolution microimaging ( $\mu\text{MRI}$ ) [4]. Another technique is decay due to diffusion in the internal field, or DDIF. DDIF was shown with *in vitro* experiments to probe surface to volume ratio [5, 6]. The present study extends DDIF to *in vivo* knee imaging.

## 2. Materials and Methods

Healthy volunteer imaging studies were conducted in a full body Siemens 3 T MRI scanner with a CP knee coil. Images were collected in the knee joint including the proximal tibia and distal femur. Protocol scans and relevant parameters are given in Table 1. High resolution anatomical images were collected with a 3D spoiled gradient echo sequence (FLASH-3D).  $T_1$  mapping used a set of inversion-prepared turbo spin echo (TSE-IR) images at variable inversion time TI.  $T_2^*$  mapping used a set of gradient echo (GRE-2D) images at variable echo times TE. DDIF images were collected with a stimulated echo + BURST readout (Figure 1) with fixed encoding time  $t_e$  and variable diffusion time  $t_D$ . Single exponential decay (or recovery) analysis generated  $T_2^*$  and  $T_{DDIF}$  (or  $T_1$  and  $M_0$ ) maps.

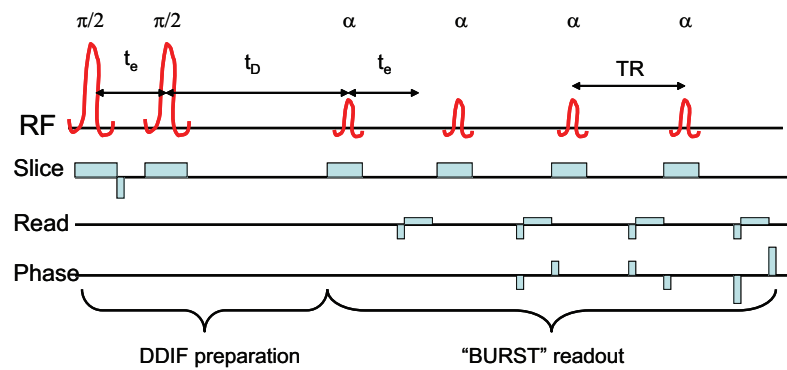


**Figure 1:** Stimulated echo prepared BURST imaging sequence used to spatially resolve DDIF contrast.

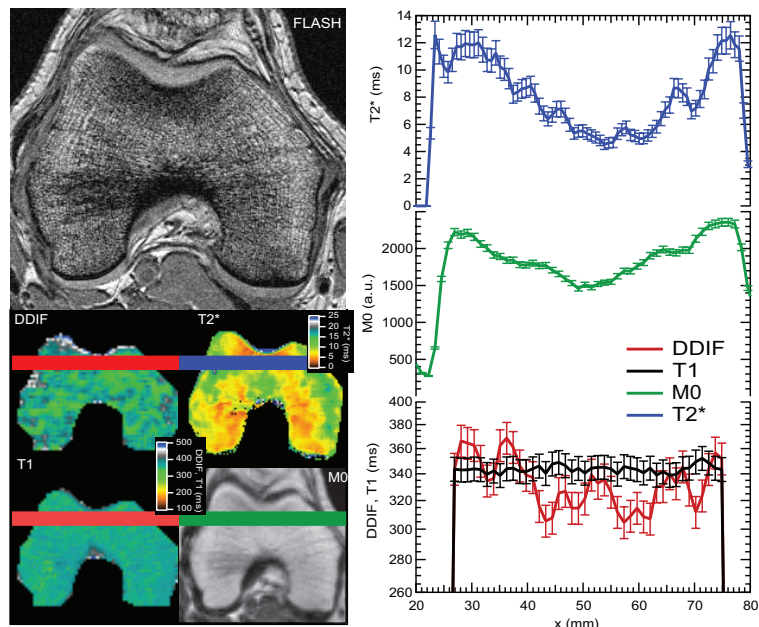
DDIF images were collected with a stimulated echo + BURST readout (Figure 1) with fixed encoding time  $t_e$  and variable diffusion time  $t_D$ . Single exponential decay (or recovery) analysis generated  $T_2^*$  and  $T_{DDIF}$  (or  $T_1$  and  $M_0$ ) maps.

Scan	Voxel(mm)	Fixed times (ms)	Variable times(ms)	$\alpha(^{\circ})$
FLASH-3D	0.3 x 0.3 x 1.5	TR/TE = 22 / 5	N.A.	30
TSE-IR	1.2 x 1.2 x 3	TR/TE = 2600 / 12	TI=23,50,100,150,200,250,300,400,500,600,700,800,900,1000	90 / 180
GRE-2D	1.2 x 1.2 x 3	TR = 642	TE=5, 7.5,10,12.5,15,17.5,20	25
DDIF	1.2 x 1.2 x 3	$t_e$ = 13,30,40,70	$t_D$ =12,50,100,150,200,250,300,400,500,600,700,1000	20

**Table 1.** 3 T MRI protocol parameters.

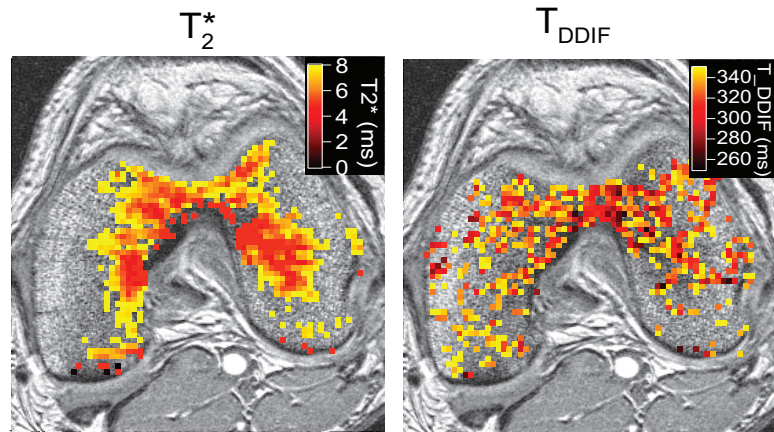
## 3. Results

Figure 2 shows imaging results for this study. High resolution FLASH images provide anatomical reference and also possess sufficient resolution to qualitatively resolve the local trabecular structure. Spin density ( $M_0$ ) maps show a lower resolution view of similar contrast.  $T_1$  maps are spatially uniform across the knee joint, reflecting the homogeneity of the bone marrow properties in comparison with the heterogeneous variation in trabecular structure.  $T_2^*$  and DDIF maps are spatially variable, reflecting variations in trabecular structure across the knee joint. DDIF decay time



**Figure 2:** Example imaging results from a healthy volunteer distal femur at 3 T. Images include high resolution anatomical reference (FLASH) and parametric maps of  $T_1$ ,  $T_2^*$  and DDIF ( $t_e = 30$  ms) decay times, as well as total magnetization  $M_0$ . Right: Line profiles (3.6 mm width) near anterior rim; error bars reflect fit precision.

values are also observed to have an upper limit that is similar to the measured spin-lattice relaxation time  $T_1$ , consistent with the background relaxation superimposed on the DDIF decay mechanism. Some correlation between variations in the  $T_2^*$  and DDIF maps is evident. For example, near the anterior rim of the distal femur in Figure 2, the  $M_0$ ,  $T_2^*$  and DDIF maps all show local minima driven by the high trabecular density and consequent strong internal



**Figure 3:**  $T_2^*$  and  $T_{\text{DDIF}}$  ( $t_e = 40$  ms) contrast in an axial slice of a healthy volunteer distal femur at 3 T. Windowed parameter maps are overlaid on a high resolution FLASH image.

field gradients. However, the precise textures of the  $T_2^*$  and DDIF maps are different both in relative quantitative magnitude and qualitative appearance. Figure 3 shows another comparison of  $T_2^*$  and DDIF ( $t_e = 40$  ms) contrast in a volunteer femur. Windowed parameter maps showing the lowest decay times (i.e. strongest contrast) in each case are overlaid on high resolution FLASH images. Both maps highlight similar territory in the intercondylar notch, where mechanical stresses and trabecular densities are high. However, the spatial patterns are not equivalent, suggesting distinct structural sensitivities.

#### 4. Discussion

Previous *in vitro* work had shown the potential of DDIF for monitoring trabecular bone structure [5], but the physiological conditions of lower diffusivity and faster spin relaxation in bone marrow compared to water could conceivably have prevented its application. The results of the present study indicate that while the DDIF contrast is quantitatively reduced, the mechanism is observable *in vivo* at 3 T. The qualitative similarity of high contrast regions of DDIF with  $T_2^*$  support its sensitivity to properties of trabecular structure, while their textural differences suggest DDIF may possess a distinct structural sensitivity. One possibility is that the surface emphasis of DDIF makes it a more specific measure of trabecular number [6]. The BURST readout used for obtaining DDIF images possessed a low signal-to-noise ratio (SNR). Future work will employ a higher SNR sequence to optimize clinical application.

#### 5. Conclusions

This study extends the DDIF contrast mechanism to *in vivo* trabecular bone for the first time in a clinical scanner. DDIF contrast showed spatial variations, superimposed on a uniform  $T_1$  background, reflecting trabecular structure. Strong contrast areas in  $T_2^*$  and DDIF maps were correlated, supporting DDIF's sensitivity to trabeculae, but textural differences suggest distinct structural sensitivities.

#### 6. References

1. Wolff, J., *Das Gesetz der Transformation der Knochen*. 1892, Berlin: A. Hirschwald.
2. Ma, J., *JMR*, 1996. **111**: p. 61-69.
3. Bouchard, L.S., *JMR*, 2005. **176**: p. 27- 36.
4. Wehrli, F.W., *NMR in Biomed.*, 2006. **19**(7): p. 731-764.
5. Sigmund, E.E. *MRM*, 2008. **59**(1): p. 28-39.
6. Sigmund, E.E., *NMR in Biomed.*, 2008, //dx.doi.org/10.1002/nbm.1354.